THE ASTRONOMICAL JOURNAL, 115:316–324, 1998 January

EXTREME ULTRAVIOLET EXPLORER RIGHT ANGLE PROGRAM OBSERVATIONS OF COOL STARS

D. J. CHRISTIAN
Center for EUV Astrophysics, 2150 Kittredge Street, University of California at Berkeley, Berkeley, CA 94720-5030; damian@cea.berkeley.edu

J. J. DRAKE
Harvard-Smithsonian Center for Astrophysics, Mail Stop 3, 60 Garden Street, Cambridge, MA 02138; jdrake@cfa.harvard.edu

AND

M. MATHIOUDAKIS
Section of Astrophysics, Astronomy, and Mechanics, Department of Physics, University of Athens, GR-157 84 Zografos, Greece; mm@rigel.da.uoa.gr

Received 1997 August 21; revised 1997 September 29

ABSTRACT

The *Extreme Ultraviolet Explorer* (*EUVE*) Right Angle Program (RAP) obtains photometric data in four bands centered at ~100 Å (Lexan/B), ~200 Å (Al/Ti/C), ~400 Å (Ti/Sb/Al), and ~550 Å (Sn/SiO) during pointed spectroscopic observations. RAP observations are up to 20 times more sensitive than those in the *EUVE* all-sky survey. We present RAP observations of two dozen late-type stars: BD +03°301, BD +05°300, HR 1262, BD +23°635, BD +22°669, Melotte 25 VA 334, Melotte 25 1366, Melotte 25 59, Melotte 25 65, θ^1 Tau, V834 Tau, GJ 2037, BD −21°1074, GJ 205, RE J0532−030, GJ 9287A, HT Vir, BD +46°1944, Proxima Cen, α Cen A/B, HR 6094, HR 8883, CPD −48°10901, and HR 8964. We derive surface fluxes from the Lexan/B and Al/Ti/C count rates and cataloged *ROSAT* Position Sensitive Proportional Counter (PSPC) data. The *EUVE* surface fluxes are reasonably correlated with surface fluxes calculated from PSPC measurements. The time variability of the sources has been examined. Most of the sources show no significant variability at the 99% confidence level. Flares were detected from the K7 V star Melotte 25 VA 334, the K3 V star V834 Tau (HD 29697), and the K3 + K8 Hyades binary BD +22°669. The BD +22°669 count rate at the peak of the flare is a factor of 6 higher than the quiescent count rate, with a peak Lexan/B luminosity of 7.9×10^{29} ergs s^{-1}. The V834 Tau flare was detected in both Lexan/B and Al/Ti/C bands. The peak luminosity of the flare is 1.6×10^{29} and 8×10^{28} ergs s^{-1} for Lexan/B and Al/Ti/C, respectively.

Key words: stars: late-type — ultraviolet emission

1. INTRODUCTION

Surveys of the sky at UV and X-ray wavelengths have revealed the universal presence of a solar-like transition range and coronal plasma in the outer atmospheres of late-type dwarfs from spectral types mid-F to late M, and in late-type giants down to mid-K (see, e.g., Vaiana et al. 1981; Jordan & Linsky 1987). Although much progress has been made toward our understanding of coronal activity in late-type stars as the result of observations with spaceborne instrumentation at UV, EUV, and X-ray wavelengths, the underlying physical mechanisms that heat their coronae to multimillion-kelvin temperatures, as well as the dynamo mechanisms themselves believed to generate the confining magnetic fields, which in turn are probably responsible for some of the heating, remain poorly understood.

While studies of the solar corona can reveal details on small spatial scales and at high spectral resolution, studies of large samples of stars enable us to explore the wide range of parameter space over which coronae form. In this regard, the surveys of the sky at EUV and X-ray wavelengths, yielding detections of stellar coronal emission over the full range of late spectral types and activity levels, are of particular interest.

The *Extreme Ultraviolet Explorer* (*EUVE*), which covers the wavelength range 58–740 Å in four filters, has provided a valuable addition to the observational database through its all-sky survey and subsequent observations. The EUV spectral range is rich in emission lines from a wide range of charge states of different elements. Indeed, the radiative losses in the EUV are comparable to X-ray losses and are important in the energy balance of stellar coronae (see, e.g., Mathioudakis et al. 1995). The *EUVE* all-sky survey yielded 275 detections of late-type stars (Bowyer et al. 1996); Lampton et al. (1997) present an additional 81 late-type stars in their catalog of fainter *EUVE* detections.

Since the initial phase of the all-sky survey was completed, *EUVE* has been dedicated to Guest Observer pointed observations, primarily using the EUV Deep Survey and Spectrometer (DSS) telescope. However, pseudoserendipitous observations of late-type stars and other objects have continued through this phase by using the survey telescopes in what has become known as the Right Angle Program (RAP; described in more detail below). The results from the first year of this program were presented by McDonald et al. (1994). One of the key advantages of RAP observations over the all-sky survey is that exposure times for each field observed on the sky are generally much longer because they are dictated by the DSS pointings. Consequently, the RAP is often up to 20 times more sensitive than the all-sky survey.

In this paper, we present an analysis of *EUVE* RAP observations of two dozen late-type stars. The relatively long RAP pointings have enabled us to study the time variability of each of these sources. We discuss the results of this analysis and we also compare our EUV observations with X-ray fluxes obtained by the *ROSAT* Position Sensi-

tive Proportional Counter (PSPC) during its all-sky survey. This paper deals primarily with the observational data; in a future paper we will analyze and discuss these results further, in the light of a larger sample of EUV detections of late-type stars and with regard to the physics of stellar coronae in general.

2. OBSERVATIONS

The *EUVE* instruments have been described in detail by, e.g., Bowyer & Malina (1991) and Malina et al. (1994). In brief, the *EUVE* broadband imaging all-sky survey telescopes (also known as "scanners") are mounted at right angles to the Deep Survey and Spectrometer instruments. During pointed observations with the DSS, these scanners can be configured to accumulate data throughout the duration of each spectrometer observation. Two of the three scanning telescopes each have a Lexan/boron ("Lexan/B") filter with a bandpass covering 58–174 Å and an Al/Ti/C filter covering 156–234 Å. The third scanning telescope has a Ti/Sb/Al filter that covers the 345–605 Å bandpass and an Sn/SiO filter covering 500–740 Å (see, e.g., Malina et al. 1994).

In the RAP, the direction in which the scanning telescopes are pointed depends on two factors: the direction of the DSS observation and the roll angle of the spacecraft. While, for a given DSS observation, the former of these is fixed, there is often considerable latitude in the choice of the latter. Based on this latitude, the roll angle can be chosen such that the scanners can acquire any interesting targets that might lie within the allowed scanner ranges of view.

Since the RAP pointings are pseudoserendipitous, we have been fortunate in that the resulting data contain a good number of observations of late-type stars. Exposure times for "good" data (spacecraft nighttime data with no Earth blockage and with periods spent passing through the South Atlantic Anomaly removed) for our star sample ranged from 18 to ~230 ks. The median exposure time was about 40 ks. BD +23°635 and BD +22°669 were observed for a total of about 230 ks, the longest uninterrupted segment being 98 ks. The sources observed, together with exposure times and their *EUVE* identifications, are listed in Table 1.

3. ANALYSIS

3.1. *Count Rates*

We used the *EUVE* IRAF analysis packages to convert the *EUVE* telemetry into QPOE (quick position-oriented event) files. These files are essentially a photon list remapped to the position of the source on the sky and so contain all the necessary timing information for deriving light curves.

Count rates were determined by using appropriate source and background apertures applied to scanner and Deep Survey QPOE files. Exposure times were correct for telescope vignetting, instrument dead times, and dead times in the telemetry (called "primbsching") using the IRAF EFFEXP routine in the EUV package. We present the resulting Lexan and Al/C count rates in Table 1.

We have also obtained the *ROSAT* PSPC count rates (and corresponding source names) for these sources from the *ROSAT* All-Sky Survey Bright Source Catalog (Voges et al. 1997) for the purposes of a comparative study with our *EUVE* count rates. The PSPC count rates are also listed in Table 1.

The average count rates that we have derived from the RAP data are in good general agreement with those reported by McDonald et al. (1994), which cover observations through 1994 January. These latter count rates were derived using different data products and software. The only discrepancy is α Cen, having nearly twice as many counts in this analysis than in the McDonald et al. RAP catalog. Our values are in agreement with the *EUVE* all-sky survey results (Bowyer et al. 1996). The discrepancy with the McDonald et al. results probably lies in the nature of the observation. The pointed scanner observations of α Cen were conducted during the calibration phase, and the pointing was switched between Lexan and Al/C filters every orbit. We suggest that the McDonald et al. analysis may not have correctly separated the data between the two filters, resulting in a larger exposure time and, hence, a lower count rate.

3.2. *Light Curves*

We used the XRAY.XTIMING package to create light curves from the QPOE photon event lists, and to test for variability for all sources. Generally, we found that binning the data per *EUVE* orbit provided sufficient counts for useful signal-to-noise ratio while maintaining as much temporal resolution as possible. We used the canonical values for the 92 minute *EUVE* orbit of 5500 s. In order to investigate possible variability in each source, we used the Kolmogorov-Smirnov (K-S) and Cramer–von Mises (CvM) statistical tests provided in IRAF and computed the excess variance. The K-S and CvM tests compute the observed cumulative distribution function of photon arrival times and compare this with the model cumulative distribution function for constant source intensity. For either test, the hypothesis of constant source intensity may be rejected at the confidence level C if the test statistic exceeds $1 - C$ for the appropriate distribution.

We computed the variance in excess of Poisson fluctuations for each light curve in a manner similar to that done for the sample of flare stars observed with *EXOSAT* (Pallavicini, Tagliaferri, & Stella 1990). However, we have parameterized our results in terms of the equivalent weighted rms fluctuation, which we call β. Such a parameterization is often used for X-ray binaries (Christian & Swank 1997 and references therein); β is given by the equation

$$\beta = \sqrt{(\chi_\nu^2 - 1)/\bar{I}}\,,$$

where $\bar{I}$ is the mean counts per time bin and χ_ν^2 is the reduced χ^2 for a fit to the source's intensity assuming a constant source model.

4. RESULTS

4.1. *Variability*

The main result from the variability study is that, generally, most sources did not show significant variability. In several cases there are large variations in the detector background as a result of the South Atlantic Anomaly, which cannot always be completely filtered by the software. If the results are not scrutinized carefully, such anomalies in the background can be confused with source variability. We have therefore been diligent in screening the resulting light curves for such occurrences. Results from this variability analysis, expressed in terms of the variability at the 99% confidence level from the K-S and CvM tests, and the per-

TABLE 1

EUVE RAP AND *ROSAT* DATA

SOURCE (EUVE)	OTHER NAMES	R.A. (*EUVE*)	DECL. (*EUVE*)	SPECTRAL TYPE	OBSERVATION START DATE (UT)	EXPOSURE (ks)	COUNT RATE (counts s^{-1})			*ROSAT* Name (1RXS)
							Lexan[a]	Al/C[b]	PSPC[c]	
J0211+04.3	BD +03°301, SAO 110399	02 11 52	04 23 59	K7	1993 Nov 25 0053:46	19	0.005 ± 0.001	<0.007	0.198 ± 0.044	J021157.5+042150
J0213+05.7	BD +05°300, SAO 110413	02 13 17	05 46 01	G0	1993 Nov 25 0053:47	19	0.006 ± 0.001	...	0.262 ± 0.046	J021321.6+054627
J0405+22.0	HR 1262, 39 Tau, HD 25680	04 05 26	22 02 22	G5 V	1993 Dec 3 0318:30	60	0.009 ± 0.001	0.009 ± 0.001	0.424 ± 0.051	J040520.3+220039
J0412+23.6	BD +23°635, HD 284163	04 12 00	23 38 22	K0	1993 Nov 28 0312:14	28	0.018 ± 0.001	0.004 ± 0.0005	0.576 ± 0.040	J041155.6+233822
					1993 Nov 29 0914:20	21	0.029 ± 0.001	0.006 ± 0.001		
					1993 Dec 2 0159:42	27	0.018 ± 0.001	0.005 ± 0.001		
					1993 Dec 3 0317:47	54	0.016 ± 0.0006	0.005 ± 0.0004		
					1994 Nov 12 1022:31	95	<0.024[d]	...		
J0418+23.2	BD +22°669, HD 284303	04 18 13	23 17 16	K3 + K8	1993 Nov 28 0312:00	28	0.024 ± 0.001	...	0.540 ± 0.036	J041811.1+231700
					1993 Nov 29 0914:38	21	0.018 ± 0.002	...		
					1993 Dec 2 0200:45	27	0.016 ± 0.002	...		
					1993 Dec 3 0318:11	54	0.018 ± 0.001	...		
					1994 Nov 12 1023:23	98	0.020 ± 0.001	...		
J0424+15.8	Melotte 25 VA 334	04 24 51	15 52 11	M0.5	1993 Oct 24 2105:42	56	0.010 ± 0.001	...	0.108 ± 0.16	J042448.7+155226
					1993 Oct 27 0926:37	33	0.006 ± 0.001	...		
J0425+15.5	Melotte 25 1366	04 25 51	15 30 54	M0	1993 Oct 24 2105:31	56	<0.0015	...	...	...
					1993 Oct 27 0926:46	33	0.002 ± 0.0002	...		
J0426+15.5	Melotte 25 59, HD 28034	04 26 08	15 31 01	G0	1993 Oct 24 2105:31	56	0.015 ± 0.001	...	0.141	J042606.0+153146
					1993 Oct 27 0926:46	33	0.013 ± 0.001	...		
J0427+15.5	Melotte 25 65, HD 28205	04 27 36	15 34 56	G0	1993 Oct 24 2105:34	56	0.006 ± 0.0004	...	0.075 ± 0.012	J042606.0+153146
					1993 Oct 27 0926:47	33	0.006 ± 0.0006	...		
J0428+15.9	θ^1 Tau, HD 28307	04 28 38	15 57 21	K0 IIIb	1993 Oct 24 2105:48	56	...	0.040 ± 0.003	0.794 ± 0.037	J042834.7+155721
					1993 Oct 27 0926:43	33	...	0.044 ± 0.004		
J0441+20.9	V834 Tau, HD 29697	04 41 19	20 53 52	K3 Ve	1994 Nov 20 0318:24	18	0.065 ± 0.002	0.016 ± 0.002	2.364 ± 0.075	J044119.0+205410
					1994 Nov 22 1650:58	72	0.091 ± 0.001	0.022 ± 0.001		
J0455−28.5	GJ 2037	04 55 41	−28 33 46	K3 V	1993 Nov 14 2131:53	52	0.004 ± 0.001	...	0.077 ± 0.017	J045335.1−283601
J0506−21.5	BD −21°1074	05 06 50	−21 34 41	dM2e	1993 Oct 19 0836:20	39	0.049 ± 0.002	0.020 ± 0.002	1.147 ± 0.099	J050649.5−213505
J0531−03.6	GJ 205, HD 36395	05 31 25	−03 40 04	M1.5 V	1993 Feb 13 1458:28	18	0.008 ± 0.002	...	0.196 ± 0.023	J053127.0−034013
J0532−03.0	RE J0532−030	05 32 04	−03 04 58	M V:e	1993 Feb 13 1458:31	18	0.005 ± 0.001	...	0.507 ± 0.051	J053204.3−030519
J0908−25.d8.....	GJ9287A, HD 78643	09 08 35	−25 49 37	G0/G1 V	1993 Mar 13 1339:13	229	0.003 ± 0.0003	...	...	...
J1346+05.1	HT Vir	13 46 08	05 06 39	G0	1993 Feb 25 0655:19	78	0.006 ± 0.001	...	0.423 ± 0.044	J134607.4+050657
J1413+46.3	BD +46°1944, HD 124694	14 13 56	46 21 29	G0	1993 May 19 2246:18	47	0.006 ± 0.001	...	0.160 ± 0.17	J141350.1+461926
J1430−62.6	Proxima Cen, GJ 551C	14 29 45	−62 40 33	M5 Ve	1992 Jul 20 0544:05	...	[e]	...	1.374 ± 0.111	J142947.9−624058
					1993 Apr 26 1032:25	167	0.030 ± 0.002	...		
J1439−60.8	α Cen A/B, GJ 559B	14 39 46	−60 50 10	G2/K1 V	1992 Jul 19 2105:36	19	0.412 ± 0.020	0.431 ± 0.020	3.876 ± 0.212	J143940.4−605020
J1623−39.2	HR 6094, HD 147513	16 23 57	−39 12 02	G5 V	1992 Jun 23 0836:21	31	0.053 ± 0.002	...	0.654 ± 0.045	J162401.2−391143
					1993 May 19 2246:18	47	0.058 ± 0.001	...		
					1993 Jun 30 1046:36	52	0.056 ± 0.002	...		
J2321−26.9	HR 8883, HD 220096	23 21 22	−27 00 19	G4 V	1993 Aug 23 1513:18	38	0.063 ± 0.002	...	3.258 ± 0.165	J232116.3−265912
J2330−47.3	CPD −48°10901, HD 221260	23 30 59	−47 22 57	K1/K2 V	1993 Aug 8 1028:26	52	0.002 ± 0.0002[f]	...	0.245 ± 0.043	J233050.0−472416
J2338+46.2	HR 8964, HD 222143	23 38 00	46 12 22	G5	1993 Oct 16 0446:38	96	0.015 ± 0.0005	...	0.286 ± 0.030	J233757.7+461156

NOTE.—Units of right ascension are hours, minutes, and seconds, and units of declination are degrees, arcminutes, and arcseconds (J2000.0).

[a] *EUVE* count rate in the Lexan/B band (58–174 Å, or 0.075–0.21 keV). Upper limits are 3 σ bounds.

[b] *EUVE* count rate in the aluminum/titanium/carbon band (156–234 Å, or 0.053–0.0.079 keV).

[c] *ROSAT* PSPC count rate in the 0.1–2.4 keV band, or 5–124 Å (Voges et al. 1997).

[d] Contaminated by pinhole leak.

[e] On the edge of the detector.

[f] Contaminated by filter bar.

TABLE 2

RESULTS: OBSERVED FLUXES AND VARIABILITY

SOURCE	*EUVE* OBSERVATION	VARIABILITY[a]	β[b] (%)	$B-V$[c]	log N_H[d]	FLUX (10^{-13} ergs cm^{-2} s^{-1}) Lexan[e]	Al/C[f]	PSPC[g]
BD +03°301	1993 Nov 25 0053:46	No	<24	1.04[h]	17.92	1.21	...	12.5
BD +05°300	1993 Nov 25 0053:47	No	<39	0.7	17.92	1.45	...	16.6
HR 1262	1993 Dec 3 0318:30	Yes	15 ± 5	0.62	17.35	2.1	...	26.7
BD +23°635	1993 Nov 28 0312:14	Yes	37 ± 6	1.09	19.00	6.4	4.3	36.0
	1993 Nov 29 0914:20	No	<21	...	...	10.3	6.5	...
	1993 Dec 2 0159:42	No	<32	...	...	6.4	5.4	...
	1993 Dec 3 0317:47	No	<20	...	...	5.7	5.4	...
	1994 Nov 12 1022:31	No	<36	...	...	8.5	...	...
BD +22°669	1993 Nov 28 0312:00	Yes	49 ± 5	0.98[i]	19.00	8.5	...	28.0
	1993 Nov 29 0914:38	No	<25	...	...	6.4	...	...
	1993 Dec 2 0200:45	Yes	19 ± 6	...	...	5.7	...	...
	1993 Dec 3 0318:11	Yes	37 ± 3	...	...	6.4	...	...
	1994 Nov 12 1023:23	Yes	27 ± 3	...	...	7.1	...	...
Melotte 25 VA 334	1993 Oct 24 2105:42	Yes	15 ± 7	1.42	18.74	3.0	...	7.10
	1993 Oct 27 0926:37	No	<25	...	...	1.8	...	...
Melotte 25 1366	1993 Oct 24 2105:31	No	<36	1.45	18.47	0.4	...	...
	1993 Oct 27 0926:46	No	<40	...	...	0.5	...	...
Melotte 25 59	1993 Oct 24 2105:31	No	<12	0.54	18.47	4.0	...	9.10
	1993 Oct 27 0926:46	No	<19	...	...	3.5	...	...
Melotte 25 65	1993 Oct 24 2105:34	No	<18	0.53	18.47	1.6	...	4.80
	1993 Oct 27 0926:47	No	<23	...	...	1.6	...	...
θ^1 Tau	1993 Oct 24 2105:48	No[j]	<8[j]	0.99	18.21	...	20.5	50.0
	1993 Oct 27 0926:43	No[j]	<19[j]	...	...	...	22.6	...
V834 Tau	1994 Nov 20 0308:24	No	<37	1.11	17.35	15.3	6.4	149.0
	1994 Nov 22 1650:58	Yes	21 ± 1	...	...	21.4	8.7	...
GJ 2037	1993 Nov 14 2131:53	No	<22	1.07	17.35	0.9	...	4.90
BD −21°1074	1993 Oct 19 0836:20	No	<28	1.52	18.02	11.5	9.4	73.0
GJ 205	1993 Feb 13 1458:28	No	<41	1.52	17.93	1.9	...	12.0
RE J0532−030	1993 Feb 13 1458:31	No	<31	1.41	17.93	1.2	...	31.0
GJ 9287A	1993 Mar 13 1339:13	Yes	18 ± 6	0.57	17.93	0.7	...	...
HT Vir	1993 Feb 25 0655:19	No	<16	0.55	17.35	1.4	...	26.0
BD +46°1944	1993 May 19 2246:18	Yes	16 ± 8	0.52	18.35	1.5	...	9.80
Proxima Cen	1992 Jul 20 0544:05	Yes	28 ± 2	2.0	17.35	7.1	...	84.0
α Cen A/B	1992 Jul 19 2105:36	Yes	14 ± 2	0.88	17.35	97.0	170.5	238.0
HR 6094	1992 Jun 23 0836:21	No	<14	0.62	18.47	14.0	...	42.0
	1993 May 19 2246:18	No	<10	...	...	15.3	...	...
	1993 Jun 30 1046:36	No	<12	...	...	14.8	...	...
HR 8883	1993 Aug 23 1513:18	No	<10	0.82	18.75	18.7	...	214.0
CPD −48°10901	1993 Aug 8 1028:26	No	<30	1.4	19.0	0.7	...	17.0
HR 8964	1993 Oct 16 0446:38	No	<8	0.66	18.00	3.7	...	18.0

[a] Variability from K-S and CvM tests at the 99% confidence limit for Lexan/B filter data unless otherwise noted.
[b] Percentage excess variance for Lexan/B filter data unless otherwise noted (see § 4.1); upper limits are 90% confidence levels.
[c] From Johnson 1966 unless otherwise noted.
[d] Hydrogen column densities derived from Jelinsky 1997 (see § 4.2).
[e] Lexan/B observed flux, using the Monsignori-Fossi & Landini 1994 line emissivities (see § 4.2).
[f] Aluminum/carbon observed flux (see note e).
[g] *ROSAT* PSPC observed flux (one per source; see note e).
[h] From Robertson & Hamilton 1987.
[i] From Stern, Schmitt, & Kahabka 1995.
[j] Variability measured for aluminum/carbon filter data.

centage excess variance (100β) are given in Table 2. Percentage excess variances ranged from 14% (α Cen) to 49% (BD +22°669) for sources showing significant variability. Significant flares or flarelike brightenings were detected from BD +22°669, V834 Tau, and, more marginally, Melotte 25 VA 334.

The flarelike activity of V834 Tau was detected in both the Lexan/B (100 Å) and Al/C (200 Å) bandpasses; light curves are presented in Figure 1. There was no information on the rise of the first flare (near MJD 9,678.75) of V834 Tau, because of Earth blockage. The flarelike activity is characterized by a rise amounting to a factor of 3 or so enhancement averaged over one orbital period, followed by more stochastic brightening, which is possibly caused by a series of smaller flares.

The light curves for the Lexan/B data of the Hyades binary BD +22°669 (K3 V + K8 V) are illustrated in Figure 2. A significant flarelike brightening is apparent near MJD 9,968.7; the decay time is of order one orbital period, or 1–2 hr. This is fairly typical of stellar X-ray flares in general and is thought to be determined primarily by the radiative cooling time of hot (10^6–10^7 K or more) plasma (see, e.g., Pallavicini et al. 1990). A second brightening near MJD 9,668.8 is possibly the result of a flare but is not clearly significant.

We show light curves for Lexan data of the Hyades member Melotte 25 VA 334 (M0.5 V) in Figure 3. This star is most likely a spectroscopic binary, though the period is not known (Griffin et al. 1988). Stern et al. (1994) detected it in a 40 ks PSPC pointing aimed at the Hyades. They

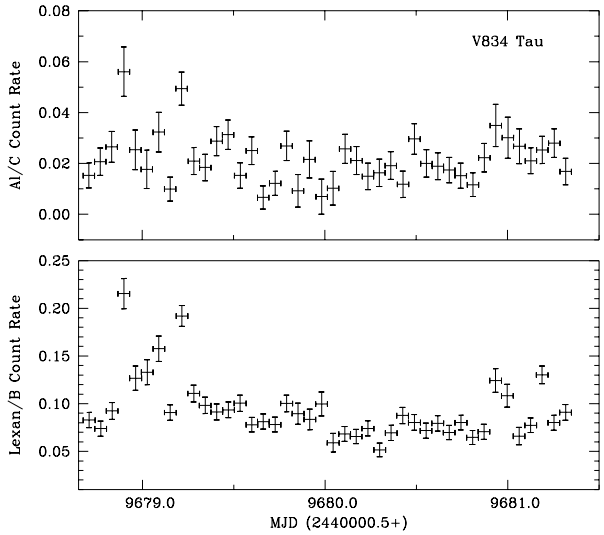

FIG. 1.—*EUVE* light curves of the November 22–27 observation of V834 Tau. *Top*, Al/C band; *bottom*, the corresponding Lexan/B band. Bin size is 5500 s (about one *EUVE* orbit).

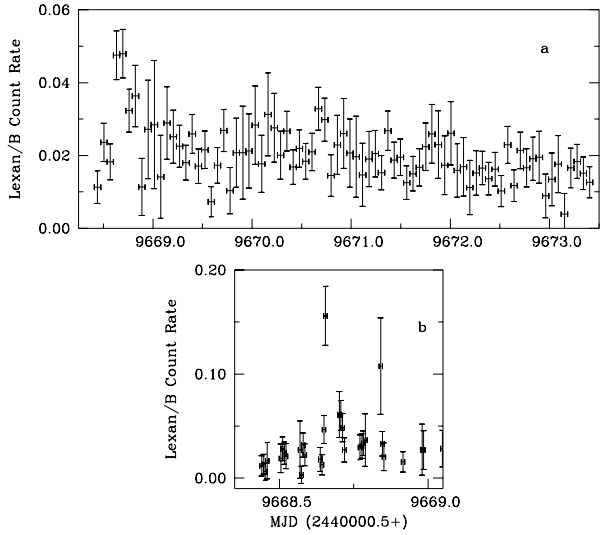

FIG. 2.—(*a*) *EUVE* Lexan/B light curve of BD +22°669 (EUVE J0418+23.2). Bin size is 5500 s. (*b*) Enlargement of the flare region in 500 s bins.

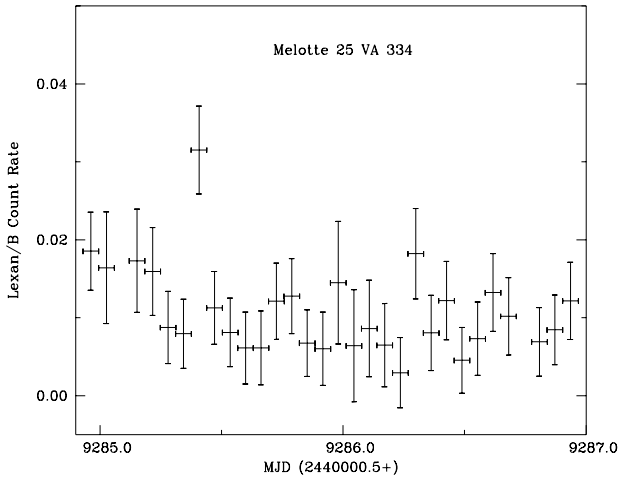

FIG. 3.—*EUVE* Lexan/B light curve of Melotte 25 VA 334. Bin size is 5500 s.

remarked that VA 334 was the only star in their Hyades sample that could be definitively said to have an X-ray flux significantly different from an earlier observation made with *Einstein* (Stern et al. 1981; Micela et al. 1988). Compared with the earlier pointing, it appeared brighter by a factor of 3 or so. Alternatively, comparison of the pointed PSPC observation and the PSPC all-sky survey yielded very similar count rates. Figure 3 shows a fairly constant count rate, within the rather large uncertainties, except for a significant flarelike brightening lasting for only one orbital period at MJD 9,285.4.

Fewer than one-third of the stars in our sampled showed short-term variability. For stars with observations separated by more than a few days count rates were similar, with the exceptions BD +23°635, BD +23°669, Melotte 25 VA 334, and V834 Tau, which showed changes of up to ~60%. We compared count rates with the *EUVE* all-sky survey (Bowyer et al. 1996) to look for longer term variability. Most sources had very similar count rates, exceptions being RE J0532−030 and HT Vir, which had twice the flux observed during the survey. V834 Tau, α Cen, Proxima Cen, HR 8883, and HR 8946 showed more modest changes of about 30%.

4.2. *Surface Fluxes*

We prefer to characterize our count rate results in terms of the stellar surface flux rather than the EUV-to-bolometric flux ratio. Other investigations have also preferred the surface flux as an appropriate parameter for studying the quiescent activity levels of late-type stars (e.g., Basri 1987; Mathioudakis et al. 1995). We have computed the observed fluxes for our sample for both our observed Lexan/B count rates and the *ROSAT* PSPC count rates using the respective instrument response functions and the line emissivities of Monsignori-Fossi & Landini (1994). We assumed a coronal plasma temperature of log $T = 6.8$, which should be fairly typical of moderately active to active stars. The results are not particularly sensitive to the assumed temperature: changing the temperature between 5×10^6 and 10^7 does not change the derived flux by more than 30%. Similar derived flux values were also obtained with the plasma emissivities of Raymond (1988).

An important parameter in converting the observed count rates to fluxes is the hydrogen column density along the line of sight. To determine the interstellar column densities, we used the model results of Jelinsky (1997), which employ a three-dimensional interpolation method on a large database of H I column densities (Fruscione et al. 1994, supplemented with additional results culled from the literature). The attenuation due to the interstellar medium was calculated using the hydrogen and helium cross sections compiled by Rumph, Bowyer, & Vennes (1994). N(H I) values ranged from 2.2×10^{17} to $\sim 10^{19}$ cm^{-2}. As found in Mathioudakis et al. (1995), Lexan/B fluxes are relatively insensitive to the choice of N(H I), except for sources with columns greater than $\sim 10^{19}$. For these sources (e.g., BD +23°635 and BD +22°669) a 50% increase in column increases the observed flux by nearly 100%.

We then converted the stellar flux received at Earth (observed flux) to stellar flux per unit radius, or surface flux. To perform this conversion we used the empirical relationship between observed flux and surface flux given by Oranje, Zwaan, & Middelkoop (1982). Bolometric corrections and effective temperatures for the conversion to

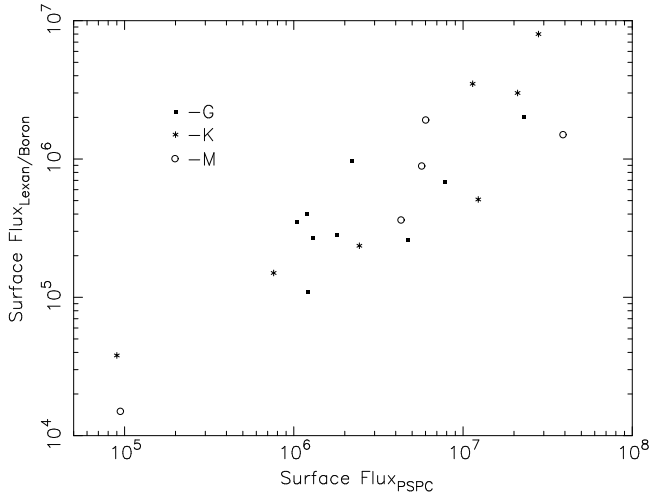

FIG. 4.—*EUVE* surface fluxes as a function of the PSPC surface fluxes, plotted on a logarithmic scale.

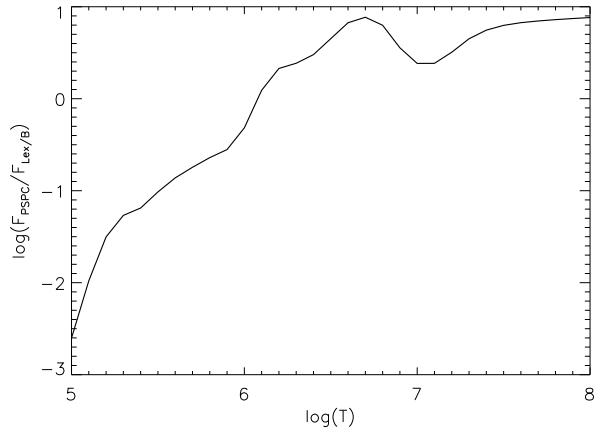

FIG. 6.—Ratio of the *EUVE* Lexan/B and *ROSAT* PSPC theoretical surface fluxes as a function of isothermal plasma temperature (see § 4.2).

surface flux were taken from Johnson (1966), using the $B-V$ or $R-I$ color of each object and corrections as discussed in Rutten et al. (1989). We present column density, $B-V$, and the derived Lexan/B and PSPC observed fluxes in Table 2.

We show the *EUVE* surface fluxes as a function of the PSPC surface fluxes in Figure 4. Generally there is good agreement, although the correlation is not as tight as results given for a sample of late-type stars detected during the *EUVE* all-sky survey and *Einstein* 3–70 Å X-ray surface fluxes (Mathioudakis et al. 1995). Possible explanations for the scatter are discussed below. In addition, we plot the *EUVE* surface fluxes as a function of $B-V$ in Figure 5. The G stars are grouped below $B-V = 0.8$, with a scatter in surface flux from 10^5 to 10^7. The K stars are grouped between $B-V = 1.0$ and 1.5 and have a large scatter in flux. The M stars are generally grouped at $B-V$ of 1.5 with similar surface fluxes, except for GJ 205 and Proxima Cen.

One potential problem with this comparison of surfaces fluxes derived from *EUVE* Lexan/B and *ROSAT* PSPC count rates is that these bandpasses are sufficiently different that there is some temperature dependence in the resulting surface flux ratios. This temperature dependence is illustrated in Figure 6, where we have plotted the ratios of the *EUVE* Lexan/B and *ROSAT* PSPC theoretical surface fluxes, derived from isothermal, optically thin plasma models, as a function of plasma temperature. In order to alleviate this problem entirely, it would be necessary to obtain mean coronal temperatures for each star, which is not feasible using our *EUVE* data alone.

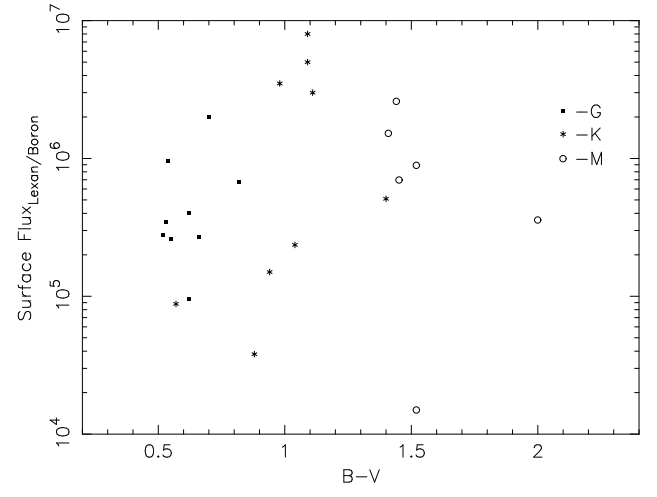

FIG. 5.—*EUVE* surface fluxes as a function of $B-V$

4.3. *Coronal Temperatures from Filter Ratios*

In the case of stars that have simultaneous detections in both Lexan/B and Al/Ti/C filters, it is possible to make a rough estimate of the average representative coronal temperature using the two filter count rates. A similar method was applied to *EXOSAT* broadband observations by Pallavicini et al. (1988) and has been discussed in detail in the context of the *EUVE* filters by Drake (1998) and by Drake et al. (1996b).

For a given plasma radiative loss model, an observed broadband count rate corresponds to a plasma emission measure, EM, for any given *isothermal* plasma temperature, T. Each filter count rate, then, when combined with a plasma radiative loss model, defines a locus in the emission measure–temperature plane. In the case of a truly isothermal plasma, the intersection of two different loci corresponding to two different filter count rates in the EM-T plane yields the plasma EM and T. In the case of stellar coronae the plasma is not likely to be isothermal, and the individual loci then represent the *upper limit* to the plasma EM at any given T. However, if the true EM distribution is relatively sharply peaked, and the bandpasses in question are largely dominated by lines formed at this peak temperature, then the isothermal approximation can be reasonable.

We have plotted the EM-T loci for the stars in our sample detected in both Lexan/B and Al/Ti/C filters in Figures 7*a*–7*e*. These stars are α Cen A/B, V834 Tau, HR 1262, BD −21°1074, and BD +23°635. In cases of multiple pointings for a given star, we have calculated the EM-T loci for the pointing with the lowest observational errors on the derived count rates. In principle, Lexan/B and Al/Ti/C flare

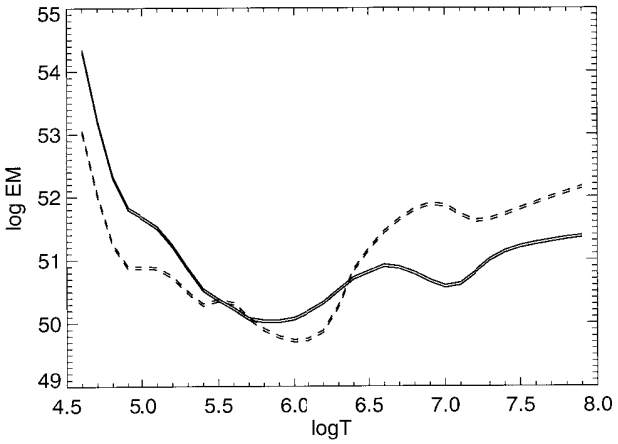

FIG. 7a

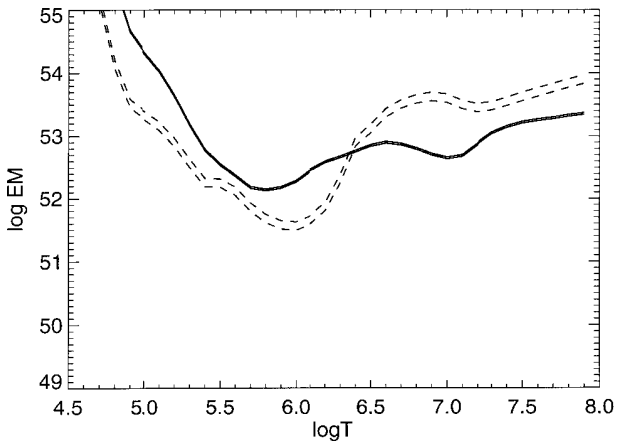

FIG. 7b

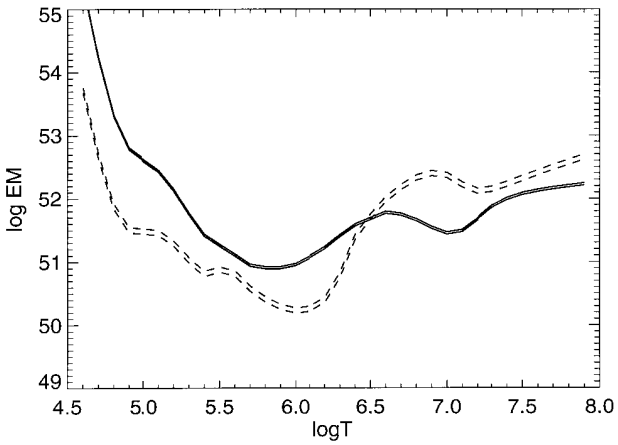

FIG. 7c

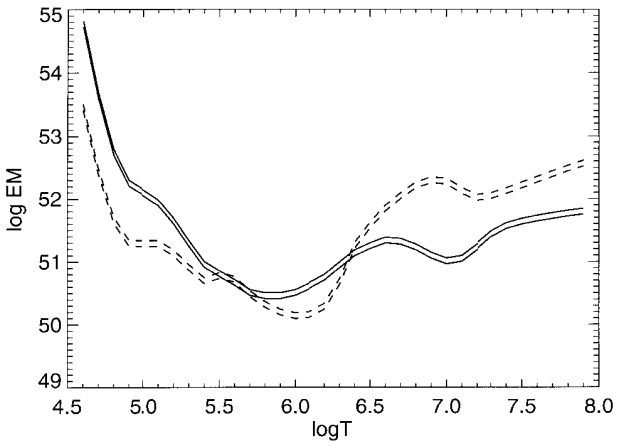

FIG. 7d

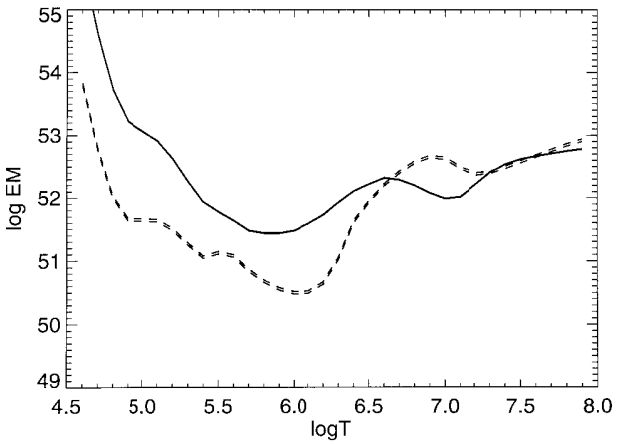

FIG. 7e

FIG. 7.—Emission measure vs. temperature "solutions" for (*a*) α Cen A/B, (*b*) BD +23°635, (*c*) BD −21°1074, (*d*) HR 1262, and (*e*) V834 Tau (see § 4.3)

light curves for, e.g., V834 Tau, could be used to estimate the rough coronal temperature as a function of time; in practice, however, the observational uncertainties on the individual points in the light curve render such an exercise of no value. In the case of the respective light curves for V834 Tau, for example, there is no significant change in the ratio of the Lexan/B and Al/Ti/C count rates as a function of time.

The intersection of the Lexan/B and Al/Ti/C loci is not always easy to interpret, since in some cases there is more than one intersection. Part of the problem stems from the fact that the two bandpasses are overlapping and not sufficiently different to provide orthogonality in the temperature index. The different stars are discussed briefly below.

α *Cen A/B.*—This system was found to be dominated 2:1 in the EUV by the B component by Drake, Laming, & Widing (1996a), in keeping with earlier X-ray measurements by Golub et al. (1982). Drake et al. (1997) have performed a detailed emission measure analysis based on individual emission lines due to different elements and find the peak

coronal temperature to be log $T = 6.3$–6.4, with an emission measure of 3×10^{50} cm^{-3}. The *EUVE* filter ratios indicate the same temperature (see Fig. 7*a*), although there is an additional intersection toward log $T = 5.6$; the emission measure is also in very good agreement with the detailed study.

BD +23°635.—This is a BY Draconis–type K3 V + K8 V close binary and Hyades member (see, e.g., Stern et al. 1992). Dempsey et al. (1997) included it in their sample of BY Draconis stars for which they studied the quiescent *ROSAT* All-Sky Survey observations, although there were apparently too few counts to perform fits to the PSPC pulse-height distribution. Our filter temperature is about log $T \sim 6.4$, which we think is too cool. Dempsey et al. (1997), for example, find the BY Draconis coronae to be dominated by the hotter of their two-temperature parameterized fits, with temperatures around log $T \sim 7$ or slightly higher. We note that the *EUVE* Al/Ti/C bandpass is much more sensitive to the log $T \sim 6.4$ range than to the log $T \sim 7$ range. The former corresponds roughly to the temperature of the cooler of the two temperature components found by Dempsey et al. (1997) in their two-temperature fits. While this cooler temperature generally has a lower emission measure, by about a factor of 3, in the Dempsey et al. (1997) fits, its contribution to the *EUVE* Al/Ti/C count rate will dominate that of the hotter component. What we are seeing, then, is the breakdown of the isothermal approximation upon which the Lexan/B-Al/Ti/C temperature estimate is based for the case of hotter coronae that have significant amounts of cooler plasma (see Fig. 7*b*).

BD −21°1074.—This star was confirmed as an EUV source by the *ROSAT* Wide Field Camera optical identification program (Mason et al. 1995). Our filter analysis suggests a coronal temperature of about log $T \sim 6.5$, but again we suspect that this might be too cool for its classification as an M2 Ve star. The active M dwarfs typically have coronal temperatures somewhat higher than this, closer to or exceeding log $T \sim 7$ (see, e.g., Schmitt et al. 1990). However, Schmitt et al. (1990) do note that the M dwarfs tend also to have significant amounts of cooler material, with temperatures of log $T \sim 6.5$, based on their analysis of the *Einstein* IPC observations. We therefore suspect that the comments made above regarding the "breakdown" of the isothermal approximation for BD +23°635 also apply here to BD −21°1074 (see Fig. 7*c*).

HR 1262 (39 Tau).—This is a G5 dwarf rotating somewhat more rapidly than the Sun, with a rotational period of 12.3 days. It was detected by *Einstein* and was included in the sample of late-type stars analyzed by Schmitt et al. (1990). It was also included in the study of rotation versus activity based on EUV fluxes by Mathioudakis et al. (1995). The count rate derived by Mathioudakis et al. (1995) from the *EUVE* all-sky survey was almost 3 times larger than the observation presented here. Schmitt et al. (1990) obtained an isothermal fit to the IPC pulse-height distribution of log $T = 6.46$ and an emission measure of log EM (cm^{-3}) = 51.2, which is in excellent agreement with our filter result (see Fig. 7*d*). The EM distribution is likely to be similar to that of the K2 dwarf ϵ Eri, which has a very similar rotational period. Laming, Drake, & Widing (1996) have recently performed a detailed line analysis based on *EUVE* spectroscopic observations and find an emission measure distribution that is more sharply peaked than that of the Sun, peaking at log $T = 6.4$–6.5.

V834 Tau.—This star was also detected in the *EUVE* all-sky survey (Bowyer et al. 1996) at a count rate of 0.125 ± 0.015 counts s^{-1}—significantly higher than the count rates determined for the RAP observations in this study. The system is a noted to be chromospherically active with strong Ca II H and K emission (Henry, Fekel, & Hall 1995 and references therein). Henry et al. discuss the possibility that V834 Tau is an undiscovered binary, possibly of the BY Draconis type. Henry et al. also present a possible 4 day period for the system, which the 3 day duration of the *EUVE* observation cannot confirm. The emission measure distribution, presented in Figure 7*e*, shows a relatively large emission measure (log EM > 52) and temperature (log $T = 6.7$–7.2), supporting the high level of activity observed for this source.

4.4. *Flare Energetics*

We have examined the energetics of the flares discussed in § 3.1. Flares were detected from the K3 V star V834 Tau (HD 29697) and the Hyades binaries BD +22°669 and Melotte 25 VA 334. The BD +22°669 count rate at the peak of the flare is approximately a factor of 6 higher than the quiescent count rate, with a peak Lexan/B luminosity of 7.9×10^{29} ergs s^{-1}. We estimate the total flare energy to be of order 10^{33} ergs. The V834 Tau flare was detected in both Lexan/B and Al/Ti/C bands. The peak luminosities of the flare are 1.6×10^{29} and 8×10^{28} ergs s^{-1} for Lexan/B and Al/Ti/C, respectively. The corresponding flare energies are of order $\sim 5 \times 10^{32}$ and $\sim 10^{32}$ ergs for Lexan/B and Al/Ti/C, respectively. Flare energies derived here for V834 Tau and BD +22°669 are in good agreement with those derived by Pallavicini et al. (1990) for a sample of nearby flare stars observed with *EXOSAT*.

5. SUMMARY

We have presented *EUVE* photometric observations for two dozen late-type stars ranging in spectral class from dG0 to dM5. Correlations of the *EUVE* surface fluxes with *ROSAT* PSPC surface fluxes and correlations with the color excess are similar to those of the *EUVE* all-sky survey data (e.g., Mathioudakis et al. 1995). Generally, most sources showed no variability on timescales shorter than the duration of the *EUVE* observations. Coronal temperatures derived from an emission measure analysis were in agreement with previous soft X-ray results for α Cen A/B and HR 1262, but ambiguous for BD +23°635 and BD −21°1074. Emission measures and temperatures derived for V834 Tau agree with the EUV activity reported here and on the basis of Ca II H and K measurements. Flares were detected from three stars: the K3 V star V834 Tau (HD 29697) and the K0 stars BD +22°669 and Melotte 25 VA 334.

We wish to thank Keh-Cheng Chu for his superb programming support in accessing the *EUVE* telemetry database. This research was partially supported by NASA Astrophysical Data Products grant NAG 5-3470 and NASA contract NAS 5-30180. J. J. D. was supported by NASA *AXAF* Science Center contract NAS 8-39073.

REFERENCES

Basri, G. 1987, ApJ, 316, 377
Bowyer, S., Lampton, M., Lewis, J., Wu, X., Jelinsky, P., & Malina, R. F. 1996, ApJS, 102, 129
Bowyer, S., & Malina, R. F. 1991, in Extreme Ultraviolet Astronomy, ed. R. F. Malina, & S. Bowyer (Elmsford, NY: Pergamon), 391
Christian, D. J., & Swank, J. H. 1997, ApJS, 109, 177
Dempsey, R. C., Linsky, J. L., Fleming, T. A., & Schmitt, J. H. M. M. 1997, ApJ, 478, 358
Drake, J. J. 1998, in preparation
Drake, J. J., Laming, J. M., & Widing, K. G. 1996a, in UV and X-Ray Spectroscopy of Astrophysical and Laboratory Plasmas, ed. K. Yamashita & T. Watanabe (Tokyo: Universal Acad.), 267
———. 1997, ApJ, 478, 403
Drake, J. J., Stern, R. A., Stringfellow, G., Mathioudakis, M., Laming, J. M., & Lambert, D. L. 1996b, ApJ, 469, 828
Fruscione, A., Hawkins, I., Jelinsky, P., & Wiercigroch, A. 1994, ApJS, 94, 127
Golub, L., Harnden, F. R., Pallavicini, R., Rosner, R., & Vaiana, G. S. 1982, ApJ, 253, 242
Griffin, R. F., Gunn, J. E., Zimmerman, B. A., & Griffin, R. E. M. 1988, AJ, 96, 172
Henry, G. W., Fekel, F. C., & Hall, D. S. 1995, AJ, 110, 2926
Jelinsky, P. 1997, in preparation
Johnson, H. L. 1966, ARA&A, 4, 193
Jordan, C., & Linsky, J. L. 1987, in Exploring the Universe with the *IUE* Satellite, ed. Y. Kondo & W. Wamsteker (Dordrecht: Reidel), 259
Laming, J. M., Drake, J. J., & Widing, K. G. 1996, ApJ, 462, 948
Lampton, M., Lieu, R., Schmitt, J. H. M. M., Bowyer, S., Voges, W., Lewis, J., & Wu, X. 1997, ApJS, 108, 545
Malina, R. F., et al. 1994, AJ, 107, 751
Mason, K. O., et al. 1995, MNRAS, 274, 1194
Mathioudakis, M., Fruscione, A., Drake, J. J., McDonald, K., Bowyer, S., & Malina, R. F. 1995, A&A, 300, 775
McDonald, K., Craig, N., Sirk, M. M., Drake, J. J., Fruscione, A., Vallerga, J. V., & Malina, R. F. 1994, AJ, 108, 1843
Micela, G., Sciortino, S., Vaiana, G. S., Schmitt, J. H. M. M., Stern, R. A., Harnden, F. R., Jr., & Rosner, R. 1988, ApJ, 325, 798
Monsignori-Fossi, B., & Landini, M. 1994, Sol. Phys., 152, 81
Oranje, B. J., Zwaan, C., & Middelkoop, F. 1982, A&A, 110, 30
Pallavicini, R., Monsignori-Fossi, B., Landini, M., & Schmitt, J. H. M. M. 1988, A&A, 191, 109
Pallavicini, R., Tagliaferri, G., & Stella, L. 1990, A&A, 228, 403
Raymond, J. C. 1988, in Hot Thin Plasmas in Astrophysics, ed. R. Pallavicini (NATO ASI Ser. C, 249) (Dordrecht: Kluwer), 109
Robertson, T. H., & Hamilton, J. E. 1987, AJ, 93, 959
Rumph, T., Bowyer, S., & Vennes, S. 1994, AJ, 107, 2108
Rutten, R. G. M., Schrijver, C. J., Zwaan, C., Duncan, D. K., & Mewe, R. 1989, A&A, 219, 239
Schmitt, J. H. M. M., Collura, A., Sciortino, S., Vaiana, G. S., Harnden, F. R., Jr., & Rosner, R. 1990, ApJ, 365, 704
Stern, R. A., Pye, J. P., Hodgkin, S. T., Stauffer, J. R., & Simon, T. 1994, ApJ, 427, 808
Stern, R. A., Schmitt, J. H. M. M., & Kahabka, P. T. 1995, ApJ, 448, 683
Stern, R. A., Schmitt, J. H. M. M., Rosso, C., Pye, J. P., Hodgkin, S. T., & Stauffer, J. R. 1992, ApJ, 399, L159
Stern, R. A., Zolcinski, M.-C., Antiochos, S. K., & Underwood, J. H. 1981, ApJ, 249, 647
Vaiana, G. S., et al. 1981, ApJ, 245, 163
Voges, W., et al. 1997, A&A, in press